Proceedings of the Estonian Academy of Sciences,
2015, **64**, 3S, 422–429
doi: 10.3176/proc.2015.3S.13
Available online at www.eap.ee/proceedings

NONLINEAR WAVES

A fresh look on old analytical solutions for water waves on a constant slope

Shanshan Xu[a*] and Frédéric Dias[a,b]

[a] School of Mathematical Sciences, University College Dublin, Belfield, Dublin 4, Ireland
[b] CMLA, UMR 8536 CNRS, Ecole Normale Supérieure de Cachan, Cachan, France

Received 5 January 2015, accepted 8 June 2015, available online 28 August 2015

Abstract. The first studies of water waves climbing a beach of constant slope were restricted to standing wave solutions. They all used potential flow theory. Various methods can be found in the literature. Hanson (The theory of ship waves. *Proc. Roy. Soc. Lond. A Mat.*, 1926, **111**, 491–529) and Stoker (*Water Waves*. Interscience, New York, 1957) gave the standing wave solution for slope angles of $\pi/2n$ with n an integer. Stoker (*Water Waves*. Interscience, New York, 1957), Peters (Water waves over sloping beaches and the solution of a mixed boundary value problem for $\triangle^2\phi - k^2\phi = 0$ in a sector. *Commun. Pur. Appl. Math.*, 1952, **5**, 87–108), and Isaacson (Water waves over a sloping bottom. *Commun. Pur. Appl. Math.*, 1950, **3**, 11–31) provided solutions for beaches of arbitrary slope angles. Due to the lack of numerical tools at the time, results were completely based on the theory of functions of complex variables, which is sometimes tedious and not easy to compare with modern numerical evaluation of analytical solutions. Here, we present four old solutions of standing waves and then evaluate the analytical solutions numerically to visualize results and perform comparisons. The run-up of waves in arbitrary water depth is also discussed.

Key words: potential flow theory, standing wave, run-up, sloping beach.

1. INTRODUCTION

When considering the motion of water waves over a beach with constant slope, one may look for periodic waves, which are either standing or progressive. In the framework of potential flow theory, scientists first restricted their studies to the standing wave solution, which is bounded everywhere. Later, they realized that in order to construct a progressive wave solution, which behaves like an incident wave far offshore, they had to allow a singularity at the shoreline [1–3]. They constructed it as the superposition of two standing waves, one bounded and the other one singular at the origin. The singularity was then interpreted as representing a loss of energy in the breaking of the waves.

Various methods for finding standing or progressive wave solutions can be found in [1–4], which are completely based on the theory of functions of complex variables. They are sometimes tedious and not easy to compare with modern numerical solutions. With the development of numerical tools, we can now evaluate the analytical solutions numerically to visualize results. Here, four different solutions of standing waves are presented and visualized to perform the comparisons.

* Corresponding author, shanshan.xu@ucdconnect.ie

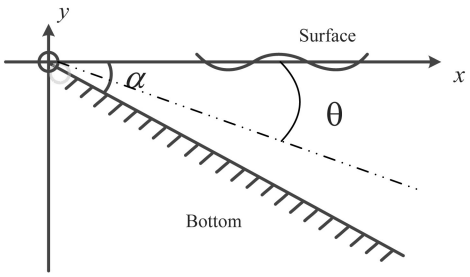

Fig. 1. Sketch of water waves on a constant slope.

Consider the nondimensional velocity potential to be in the form of $\phi^*(x^*,y^*)\cos(t^*)$ for standing waves with the bathymetry shown in Fig. 1. The conditions of the problem can be put in the form

$$\begin{aligned} \phi^*_{x^*x^*}+\phi^*_{y^*y^*} &= 0, && (1)\\ \phi^*_{y^*}-\phi^* &= 0, \qquad y^*=0, && (2)\\ \phi^*_n &= 0, \qquad z^*=r^*e^{-i\alpha}, && (3)\\ \eta^*-\phi^*\sin t^* &= 0, \qquad y^*=0, && (4) \end{aligned}$$

where

$$x^*=kx, \qquad y^*=ky, \qquad t^*=\omega t, \qquad \eta^*=\frac{\eta}{a}, \qquad \phi^*=\frac{k}{\omega a}\phi,$$

α is the angle of the slope, η is the free surface elevation, g is the acceleration due to gravity, a is the incident wave amplitude at ∞, ω is the angular frequency, $\vec{n}$ is the normal vector at the bottom, and k is the wavenumber. The wavenumber and the angular frequency satisfy the dispersion relation $\omega^2=gk$.

The various methods used to obtain the velocity potential involve a complex function $f(z^*=r^*e^{i\theta})$, with

$$\phi^*=\boldsymbol{Re}\, f, \tag{5}$$

where ***Re*** means the real part.

2. THE LINEAR STANDING WAVE SOLUTION IN DEEP WATER

2.1. The standing wave solution over beaches at angles $\alpha=\pi/2n$

Making use of the fact that the slope angle is $\pi/2n$ with n an integer, there are two solutions to construct the standing wave.

The first solution is

$$\begin{cases} f_1=A_1\exp\{r^*\sin\theta-ir^*\cos\theta\},\\ f_2=A_2\exp\{r^*\sin(-2\alpha-\theta)-ir^*\cos(-2\alpha-\theta)\},\\ f_3=A_3\exp\{r^*\sin(-2\alpha+\theta)-ir^*\cos(-2\alpha+\theta)\},\\ \cdots\cdots\cdots\\ f_{2m}=A_{2m}\exp\{r^*\sin(-2m\alpha-\theta)-ir^*\cos(-2m\alpha-\theta)\},\\ f_{2m+1}=A_{2m+1}\exp\{r^*\sin(-2m\alpha+\theta)-ir^*\cos(-2m\alpha+\theta)\}, \end{cases} \tag{6}$$

$f=\sum f_i$ and where the A_j $(j=1,\cdots,2m)$ are complex coefficients.

The second solution is

$$\begin{cases} f(z^*) = \dfrac{\pi}{(n-1)!\sqrt{n}} \displaystyle\sum_{m=1}^{n} c_m e^{z^*\gamma_m} \\ \gamma_m = \exp\left\{ i\pi \left(\dfrac{m}{n} + \dfrac{1}{2} \right) \right\} \\ c_m = \exp\left\{ i\pi \left(\dfrac{n+1}{4} + \dfrac{m}{2} \right) \right\} \cot\dfrac{\pi}{2n} \cot\dfrac{2\pi}{2n} \ldots \cot\dfrac{(m-1)\pi}{2n}, \qquad m = 2\,,3\,,\ldots,\ n \\ c_1 = \bar{c}_n. \end{cases} \tag{7}$$

As $|z^*| \to \infty$ in the sector, all terms inside the sum clearly die out exponentially except the term for $m = n$, which is $c_n \exp\{-iz^*\}$, since all γ_m's have negative real parts except γ_n. Even the term for $m = n$ dies out exponentially except along lines parallel to the real axis. Hence, the asymptotic behaviour of the real potential functions ϕ at ∞ yields

$$\phi(x^*, y^*) = \boldsymbol{Re} f \sim \frac{\pi}{(n-1)!\sqrt{n}}\, e^{y^*} \cos\left(x^* + \frac{n-1}{4}\pi \right). \tag{8}$$

This solution is uniquely determined as soon as the amplitude is prescribed at ∞ since ϕ yields the only standing wave solution of our problem.

Once we have $\phi^* = \boldsymbol{Re} f$, the free surface elevation of the incident wave can be determined by Eq. (4). The numerical values of A^* can be obtained, where $A^* = max|\eta^*(0)|/max|\eta^*(\infty)|$. From the data in Fig. 2a, the fitting curve of A^* for the first and second solutions can be described by

$$A^* = \left(\frac{\pi}{2\alpha} \right)^{1/2}. \tag{9}$$

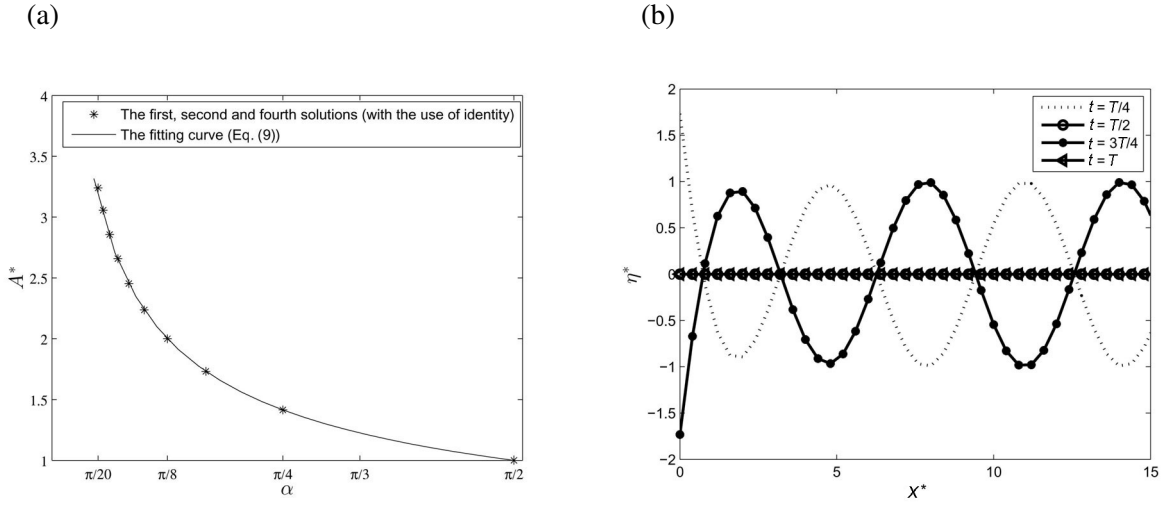

Fig. 2. Graphs of the ratio A^* for different angles of slope (a) and the nondimensional free surface elevation of the incident wave over sloping beach with the angle $\alpha = \pi/6$ at time $T/4, T/2, 3T/4$, and T (b). A^*, expressed using stars in (a) can be given by the first Eq. (6), second Eq. (7), and the fourth solutions (with the use of identity) (Eq. (10) + Eq. (13)). The solid line in (a) represents Eq. (9), which is the fitting curve of numerical values A^*. η^* in (b) shows the behaviour given by all these four solutions (Eqs (6), (7), (10) + (11), and (10) + (12)).

A graph of the free surface elevation over the sloping beach with angle $\alpha = \pi/6$ ($n = 3$), which is given by the first two solutions, is shown in Fig. 2b. It can be observed that the nondimensional free surface elevation of the incident wave behaves like $\cos(x+\psi)\sin t$ far from the shoreline, in agreement with the standing wave behaviour in water of infinite depth.

2.2. The standing wave solution for beaches of arbitrary slopes

In the previous section, the standing wave solution on the sloping beach at angle $\pi/2n$ is given. Now, the case of a beach with arbitrary slope is introduced. Again two solutions are given.

The third solution

$$f(z^*) = \frac{1}{2\pi i \|h(-i)\|} \int_P e^{\varsigma z^*} \frac{h(\varsigma)}{\varsigma + i} d\varsigma, \tag{10}$$

where the function $h(\varsigma)$ is defined by

$$h(\varsigma) = \exp\left\{ \frac{1}{2\pi i} \int_{-\infty}^{0} \frac{\log\left[\dfrac{\xi^{\alpha/\pi} + ie^{-2i\alpha}}{\xi^{\alpha/\pi} - i}\right]}{\xi - \varsigma^{\pi/\alpha}} d\xi \right\}, \tag{11}$$

and the path P is symmetric with respect to the real axis (Fig. 3).

The fourth solution.

The function $h(\varsigma)$ can be also expressed as

$$h(\varsigma) = \exp\left\{ \frac{1}{\pi i} \int_{i\infty}^{-i\infty} \frac{\log\left(\dfrac{|\xi|^{\pi/\alpha}}{|\xi|^{\pi/\alpha} - 1} \cdot \dfrac{|\xi|^2 - 1}{|\xi|^2}\right)^{1/2}}{\xi - \varsigma} d\xi \right\}. \tag{12}$$

Meanwhile, the expression for $h(\varsigma)$ can be simplified for the special values of angle $\alpha = p\pi/2q$, where p is odd, by using an identity. The resulting expression, denoted by h_I, is

$$h_I(\varsigma) = \frac{\varsigma^{\frac{q}{p}-1} \prod_{k=1}^{(p-1)/2} \left(\varsigma^{2q/p} - \exp\{i\pi(4k-1)q/p\}\right)}{\prod_{j=1}^{q-1} \left(\varsigma - \exp\{i\pi(jp/q + 1/2)\}\right)}. \tag{13}$$

In theory, the ratio A^* and the free surface elevation should coincide with the behaviours shown in Fig. 2. However, the path integrals in the complex plane of these two solutions are complicated and difficult to calculate. With the development of numerical tools, we can now evaluate and visualize them numerically. The function "NIntegrate" in Mathematica is a general numerical integrator, which estimates the integral through sampling of integrand values over the integration region. The numerical results of the third and fourth solutions reproduce the wave elevation accurately, except near the origin. The smaller the slope angle, the more singularities there are at the origin, which leads to numerical errors. A^* calculated by the fourth solution (Eq. (10) + Eq. (12)) is plotted in Fig. 4. It matches the fitting curve of Eq. (9) well as long as the slope angle is not too small. When A^* is calculated by the fourth solution with the use of identity (Eq. (10) + Eq. (13)) that avoids complex integrals, it coincides with the result given by the fitting curve (see Fig. 2a).

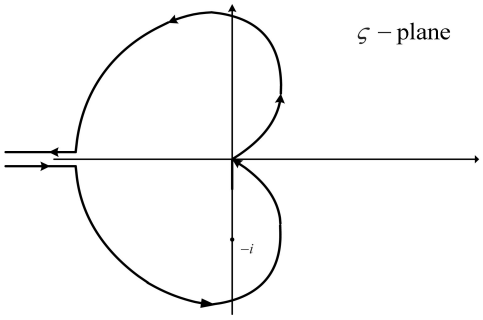

Fig. 3. The path P in the complex plane.

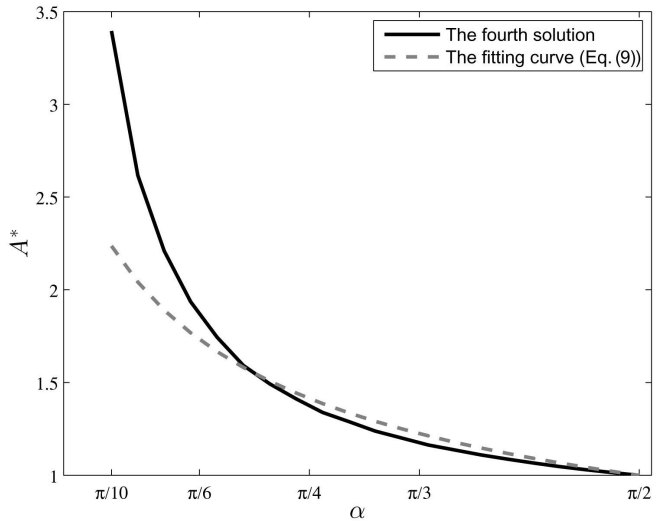

Fig. 4. Graph of the ratio A^* for different slope angles. The black solid line represents the solution A^* given by the fourth solutions (Eq. (10) + Eq. (12)). The dashed red line represents the fitting curve for A^* (Eq. (9)).

3. WAVE RUN-UP IN ARBITRARY WATER DEPTH

For the life cycle of a wave, run-up is an important indicator to be measured. Run-up has two different definitions. In the linear potential flow theory, we assume that the amplitude of the disturbance of the free surface is much less than the water depth. Then the motion becomes a small perturbation of the equilibrium position in which the surface is given by $y = 0$, and the shoreline is fixed at $x = 0$. The run-up is then defined as the wave amplitude at origin. In nonlinear theory, the run-up of the wave is the maximum vertical extent of wave up-rush on a beach or a structure above the still water level. The moving shoreline is defined by $h + \eta = 0$, where h is the still water depth.

The four solutions above are only valid in deep water (the dispersion relation $k = \omega^2/g$ has been used). Under the assumption of the standing wave solution, the incident wave is assumed to be fully reflected from the shore and an equivalent outgoing wave is added. The run-up in deep water in linear theory can be expressed by

$$R = 2A^* a = a\left(\frac{2\pi}{\alpha}\right)^{1/2}. \tag{14}$$

While linear theory is a good approximation in the far-field, where waves propagate in deep water, it is obvious that nonlinearity plays an important role during the run-up process. The nonlinear shallow water equations are considered to solve this problem. There are plenty of papers providing solutions of these equations, such as [5–7]. The free surface elevation is provided for example by Madsen and Fuhrman [8]:

$$\eta(\rho,\lambda) = RJ_0(\omega\rho)\cos(\omega\lambda) - \frac{u^2}{2g}, \tag{15}$$

where J_0 is the Bessel function of the first kind,

$$\lambda = t - \frac{u}{g\alpha}, \tag{16}$$

$$\rho = \frac{2\sqrt{g(H+\eta)}}{g\alpha}, \tag{17}$$

$$\psi(\rho,\lambda) = -\frac{2R}{\alpha\omega}J_0(\omega\rho)\sin(\omega\lambda), \tag{18}$$

$$u(\rho,\lambda) = \frac{1}{\rho}\frac{\partial\psi}{\partial\rho}. \tag{19}$$

The run-up R is in agreement with the linear shallow water result, which can be described by

$$R = 2a\sqrt{\frac{\pi}{\alpha}}\left(\frac{h_0\omega^2}{g}\right)^{1/4}, \tag{20}$$

where h_0 is the initial water depth. Figure 5 shows the free surface elevation in nonlinear shallow water and Fig. 6a gives plots of Eq. (14) and Eq. (20), which present the run-up of the wave in deep and shallow water. As the minimum run-up is 2 as indicated in [8], Eq. (20) is only valid when the slope angle is small, which is consistent with the assumption of shallow water.

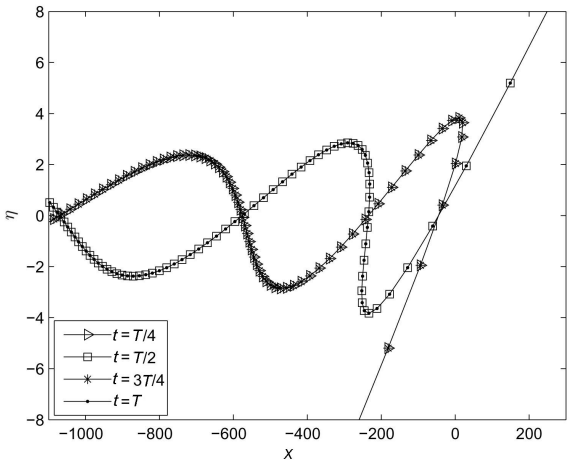

Fig. 5. The free surface elevation for nonlinear shallow water using Eq. (15) at time $T/4, T/2, 3T/4, T$, and period $T = 20\pi$. The slope angle $\alpha = \pi/100$ and the incident wave amplitude $a = 1$ m at the depth $h_0 = 50$ m.

The run-up in intermediate water can be expressed by [9]

$$R = a\left(\frac{2\pi}{\alpha}\right)^{1/2} \frac{\left(k_0 \sinh^2 \dfrac{\omega^2 k_0 h_0}{g} + \dfrac{\omega^2 k_0 h_0}{g}\right)^{1/2}}{\cosh \dfrac{\omega^2 k_0 h_0}{g}}, \tag{21}$$

where k_0 is the root of the equation

$$k_0 \tanh \frac{\omega^2 k_0 h_0}{g} = 1. \tag{22}$$

4. CONCLUSIONS

Four different solutions describing the standing wave behaviour on sloping beaches have been presented. Although the expressions are different, after applying numerical methods to visualize the results, the free surface elevation of the incident wave far from the shoreline behaves like

$$\eta = a\cos(kx + \psi)\sin\omega t.$$

The run-up of the wave can be represented by Eq. (14) in deep water when the slope angle is not small. It can be expressed by Eq. (20) in shallow water of slowing varying depth, and by Eq. (21) in intermediate water (see Fig. 6b).

The first two deep water solutions are only applicable to the case where the sloping angle $\alpha = \pi/2n$. Our numerical simulation of the third solution did not give satisfactory results near the origin. Our numerical simulation of the fourth solution is good as long as the slope angle is not too small. However, it has the highest computational cost (Fig. 7). The fourth solution with the use of the identity has the lowest cost, but it is only appropriate for the special case with slope angle $\alpha = p\pi/2q$.

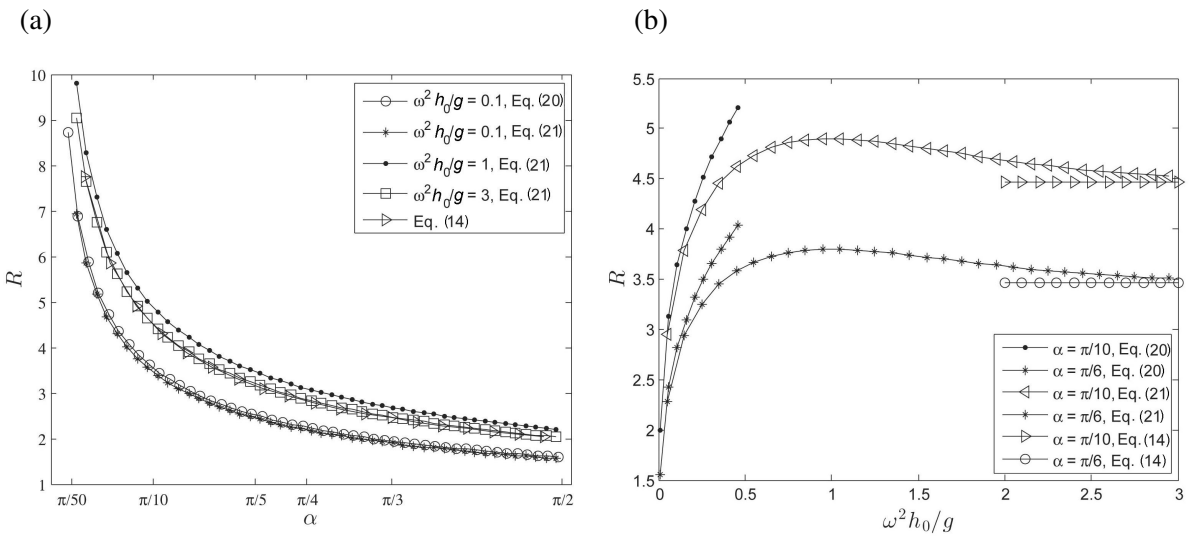

Fig. 6. Graphs of the wave run-up as a function of slope angle α (a) and of $\omega^2 h_0/g$ (b). Eqs (14), (20), and (21) represent the run-up in shallow, intermediate, and deep water, respectively. And the incident wave amplitude $a = 1$ m.

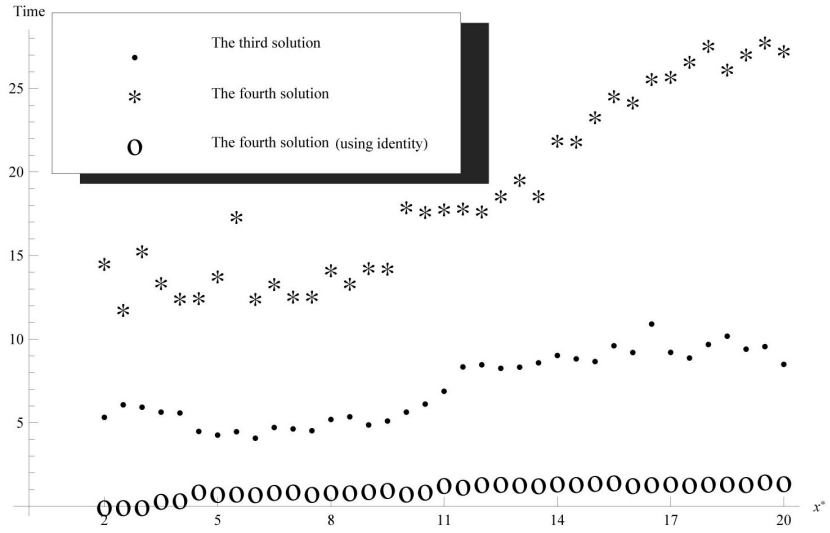

Fig. 7. The running time (in seconds) of the real part of the complex potential ϕ^* as x^* goes from 2 m to 20 m. The dots represent the third solution whose $h(\varsigma)$ is based on Eq. (11), the stars represent the fourth solution whose $h(\varsigma)$ is based on Eq. (12). The circles describe the fourth solution with the use of identity Eq. (13). The slope angle is $\pi/4$.

REFERENCES

1. Stoker, J. J. *Water Waves*. Interscience, New York, 1957.
2. Peters, A. S. Water waves over sloping beaches and the solution of a mixed boundary value problem for $\triangle^2\phi - k^2\phi = 0$ in a sector. *Commun. Pur. Appl. Math.*, 1952, **5**, 87–108.
3. Isaacson, E. Water waves over a sloping bottom. *Commun. Pur. Appl. Math.*, 1950, **3**, 11–31.
4. Hanson, E. T. The theory of ship waves. *Proc. Roy. Soc. Lond. A Mat.*, 1926, **111**, 491–529.
5. Synolakis, C. E. The runup of solitary waves. J. Fluid Mech., 1987, **185**, 523–545.
6. Carrier, G. F., Wu, T. T., and Yeh, H. Tsunami run-up and draw-down on a plane beach. J. Fluid Mech., 2003, **475**, 79–99.
7. Stefanakis, T. S., Xu, S. S., Dutykh, D., and Dias, F. Run-up amplification of transient long waves. *Q. Appl. Math.*, 2015, **73**, 177–199.
8. Madsen, P. A. and Fuhrman, D. R. Run-up of tsunamis and long waves in terms of surf-similarity. *Coast. Eng.*, 2008, **55**, 209–223.
9. Keller, J. B. and Keller, H. B. *Water Wave Run-up on a Beach*. Technical Report. Department of the Navy, Washington, DC, 1964.

Lainerünnaku keerukate analüütiliste kirjelduste numbrilise analüüsi tehnika

Shanshan Xu ja Frédéric Dias

Esimesed konstantse kaldega rannas aset leidvate lainerünnakute mudelid piirdusid seisulainete omaduste analüüsiga klassikalise keerisevaba (potentsiaalse) voolamise raames. Kirjanduses on esitatud vastav analüüs algul teatavate fikseeritud kaldenurkade ja hiljem mistahes ratsionaalarvulise kaldenurga jaoks. Formaalsed lahendused on esitatud väga keerukate avaldistena, mis tuginevad kompleksmuutuja funktsioonide spetsiifilistel omadustel, mistõttu lainerünnakute tegelike omaduste arvutamine on väga keerukas. Töös on esitatud metoodika neljale põhimõtteliselt tuntud analüütilisele lahendile vastavate füüsikaliste suuruste arvutamiseks ja visualiseerimiseks ning on määratletud erinevate lahendite rakenduspiirkonnad.